

## LETTER

## Spatial scaling of population synchrony in marine fish depends on their life history

Jonatan F. Marquez,<sup>1\*</sup> Aline Magdalena Lee,<sup>1</sup> Sondre Aanes,<sup>2</sup> Steinar Engen,<sup>3</sup>Ivar Herfindal,<sup>1</sup> Are Salthaug<sup>4</sup> andBernt-Erik Sæther<sup>1</sup><sup>1</sup>Department of Biology, Centre for Biodiversity Dynamics, Norwegian University of Science and Technology, 7491, Trondheim, Norway<sup>2</sup>Norwegian Computing Center 0314, Oslo, Norway<sup>3</sup>Department of Mathematical Sciences, Centre for Biodiversity Dynamics, Norwegian University of Science and Technology, 7491, Trondheim, Norway<sup>4</sup>Institute of Marine Research Post box 1870 Nordnes, 5817, Bergen, Norway

\*Correspondence: E-mail:

jonatan.f.marquez@ntnu.no

## Abstract

The synchrony of population dynamics in space has important implications for ecological processes, for example affecting the spread of diseases, spatial distributions and risk of extinction. Here, we studied the relationship between spatial scaling in population dynamics and species position along the slow-fast continuum of life history variation. Specifically, we explored how generation time, growth rate and mortality rate predicted the spatial scaling of abundance and yearly changes in abundance of eight marine fish species. Our results show that population dynamics of species' with 'slow' life histories are synchronised over greater distances than those of species with 'fast' life histories. These findings provide evidence for a relationship between the position of the species along the life history continuum and population dynamics in space, showing that the spatial distribution of abundance may be related to life history characteristics.

## Keywords

Abundance, generation time, modifiable areal unit problem, pace of life, population dynamics, population growth rate, slow-fast continuum life history variation, spatial processes.

Ecology Letters (2019) 22: 1787–1796

## INTRODUCTION

The complexity and scale of spatial population dynamics greatly influence population's responses to current large-scale ecological threats, such as climate change, overharvesting and fragmentation (Ellis & Schneider 2008). Population dynamics are mainly regulated by environmental variation and density (Sæther 1997). Because these regulating factors often vary in space, local population parameters (e.g. abundance, vital rates) are also expected to show spatial variation (Barraquand & Murrell 2012). However, the spatial variation of these population parameters is often spatially autocorrelated, meaning that values of population parameters at nearer locations tend to be more similar than at more distant locations (Ellis & Schneider 2008). Similarly, temporal variation in population parameters often correlates more among closer locations than distant ones, resulting in spatial synchrony patterns (Koenig 1999).

The rate at which synchrony in population parameters declines with increased distance (i.e. the spatial scaling) is of central importance in ecology (Engen 2017), for instance because the probability of global extinction increases with increased spatial scaling (Heino *et al.* 1997; Engen *et al.* 2002; Liebhold *et al.* 2004). This is because local densities in synchronised populations are more likely to all be low simultaneously, leaving the entire population vulnerable to stochastic events. Also, synchrony has been shown to influence other ecological processes, such as the rate of spread of invasive species, diseases and parasites (e.g. Ovaskainen & Cornell 2006; Kausrud *et al.* 2007; Giometto *et al.* 2017), the optimal sustainable harvesting rate (e.g. Ruokolainen 2013; Engen 2017), and the relation

between occupied range size and population growth rate (Engen 2007). While the presence of spatial synchrony has been established in a variety of systems, identifying drivers causing it has often been more elusive.

Three main processes are known to cause spatial synchrony in population dynamics (Bjørnstad *et al.* 1999; Liebhold *et al.* 2004). First, widely synchrony environmental variables, such as climate, can synchronise dynamics of local populations that have the same density regulation structure (i.e. the Moran effect: Moran 1953; Royama 1977; Grøtan *et al.* 2005). Second, widespread trophic interactions can affect spatial synchrony through, for example, the regulating effects of a common predator/parasite on the vital rates of a prey/host population (Ims & Andreassen 2000). Widespread harvesting can also induce analogous responses in the targeted species (Frank *et al.* 2016; Engen 2017; Engen *et al.* 2018). Third, individual dispersal tends to increase the distance over which population dynamics are synchronised (Ranta 1997; Paradis *et al.* 1999; Bjørnstad & Bolker 2000; Kendall *et al.* 2000). These processes often act simultaneously on a population, hindering the task of quantifying their individual effects, and are further influenced by other factors, such as cyclic population dynamics (Vasseur & Fox 2009) or by geographical patterns (e.g. topography, geographical barriers, latitudinal gradients; Walter *et al.* 2017). Population parameters, like strength of density dependence and demographic stochasticity, have also been shown to affect spatial synchrony, further complicating the identification and understanding of how spatial scaling varies among species (Lande *et al.* 1999; Engen *et al.* 2005b; Sæther *et al.* 2007; Engen 2017).

Theoretical studies have shown how several population parameters, such as strength of density regulation and population growth rate, can affect spatial synchrony (Murdoch *et al.* 1992; Lande *et al.* 1999; Bahn *et al.* 2008). Empirical studies have also identified some important extrinsic factors affecting synchrony in wild populations, such as habitat type (Paradis *et al.* 1999, 2000), weather patterns (Lindström *et al.* 1996; Ranta 1997; Grøtan *et al.* 2005) and harvesting pressure (Frank *et al.* 2016; Kuo *et al.* 2016). However, fewer intrinsic population factors have been studied empirically, with notable exceptions like dispersal strategy (Paradis *et al.* 1999; Jones *et al.* 2007), strength of density regulation and demographic stochasticity among birds (Sæther *et al.* 2007).

Finding general patterns of covariation in ecological processes is important for our understanding of population dynamics and for the development of broad conservation and harvesting strategies. One ecological simplification that has proven to be very useful is the slow-fast continuum of life histories (Jennings *et al.* 1998; Ferguson & Lariviere 2002; Engen *et al.* 2005a; Jones *et al.* 2008). Early maturing species with short generation times and high reproductive rates characterise the fast end of the continuum, while long-lived species with high adult survival represent the slower end (Sæther & Bakke 2000; Ferguson & Lariviere 2002; Oli 2004). From a species' allocation along the continuum (i.e. pace of life), other aspects of its population dynamics can be predicted (Sæther *et al.* 1996; Jennings *et al.* 1998; Jones *et al.* 2008). For example, population growth of faster lived species tends to be more sensitive to changes in fecundity rates, whereas slow lived species are more affected by changes in adult survival (Oli 2004). This general pattern has been demonstrated in wild populations of birds (Sæther & Bakke 2000), mammals (Oli 2004; van de Kerk *et al.* 2013), reptiles (Shine & Charnov 1992; Clobert *et al.* 1998) and fish (Bjørk voll *et al.* 2012; Thorson *et al.* 2017), and shown to be useful for the development of management strategies (Ferguson & Lariviere 2002).

In this paper, we examine whether the pace of life of a species, that is, its placement along the slow-fast continuum, can also predict the spatial scaling of its population synchrony. We do this by analysing spatial synchrony in two population variables – abundance and yearly change in abundance – in relation to species life history parameters that are directly related to the slow-fast continuum – population growth rate, mortality and generation time – of eight species of fish in the Barents Sea living under similar environmental conditions.

## MATERIALS AND METHODS

### Study area

We used spatial data and life history trait data from eight Barents Sea round-fish species (Fig. 1). Many of the fish stocks in the Barents Sea have been regularly monitored for decades resulting in consistent high-quality datasets with spatial information (Stiansen & Filin 2008) on species living in the same environment but covering a range of life history strategies (Bjørk voll *et al.* 2012), making the region an outstanding model to study general patterns of spatial synchrony in relation to life history. The Barents Sea is highly seasonal,

becoming largely covered during the winter period by sea ice that gradually melts during spring. Many of the fish inhabiting this sea carry out long seasonal migrations between spawning and feeding grounds (Olsen *et al.* 2010), suggesting high dispersal capabilities. Because spawning occurs largely outside of the study area and is followed by a planktonic phase (Olsen *et al.* 2010), we assume that populations give rise to synchrony through dispersal dynamics and local mortality rates, rather than self-recruitment. In other words, as local abundances fluctuate, local mortality and dispersal dynamics will be affected by density regulation processes thereby affecting abundance distribution patterns, while high reproductive rates at a specific region will not necessarily cause that region, or nearby ones, to receive a greater recruitment in the future. Nevertheless, social learning from older cohorts to younger ones has been suggested for species like herring (*Clupea harengus*; Huse 2016) and capelin (*Mallotus villosus*; Fauchald *et al.* 2006), where older cohorts lead younger ones to particular regions based on experience. This behaviour is reportedly strengthened with the abundance of the older cohort, thereby drawing an indirect link between local abundances of consecutive years. The species included in this study were: North East Atlantic (NEA) cod (*Gadus morhua*), NEA haddock (*Melanogrammus aeglefinus*), NEA saithe (*Pollachius virens*), beaked redfish (*Sebastes mentella*), golden redfish (*Sebastes marinus*), blue whiting (*Micromesistius poutassou*), Barents Sea capelin and Norwegian spring-spawning herring. All these species are subject to direct or indirect harvesting (ICES 2016).

### Estimation of population life history parameters

We used five life history parameters to characterise the species' allocation along the slow-fast continuum; population growth rate and its variability, mortality and its variability, and generation time. Species at the fast end of the continuum

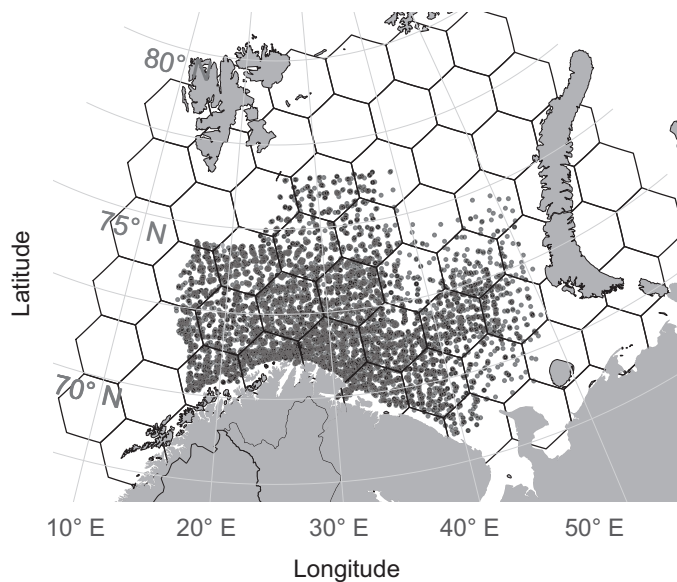


**Figure 1** Barents Sea and surrounding land masses. The study region is overlaid with the hexagonal grid with 36 100 km<sup>2</sup> areas used for the spatial synchrony analysis. Each dot represents a sampling site.

are expected to have high population growth rates, high mortality and short generation times (Sæther *et al.* 1996). Fast species are also generally expected to have more variable population dynamics than those at the slow end of the continuum (Shelton & Mangel 2011; Bjørkvoll *et al.* 2012). We therefore also included measures of variability of population growth and mortality. Estimates of life history parameters were retrieved from Bjørkvoll *et al.* (2012), where they were estimated in a Bayesian hierarchical state-space population model using data on commercial harvesting, scientific survey abundance indices and information on proportions of mature individuals at age per year (ICES 2008a, 2008b, 2009). Detailed information of the data from Bjørkvoll *et al.* (2012) can be found in Appendix S1 and in their supplementary materials.

Generation time ( $GT$ ) was defined as the mean age of mothers of newborn individuals, assuming a stable age distribution. Mortality was estimated as the expected natural mortality rate across ages and years,  $E(M_{a,t})$ , starting from the age at which individuals are recruited into the fishery and excluding the mortality caused by harvesting (for a full description of their methodology see Appendix S1 and Aanes *et al.* (2007); Bjørkvoll *et al.* (2012)). The variance of mortality,  $\text{Var}(M_{a,t})$ , was estimated using the standard formula for the variance of the log-normal distribution. The annual multiplicative population growth rate,  $\lambda_t$ , represented the potential population growth in the absence of harvesting. Variation in the growth rate among years was included by calculating the coefficient of variation,  $\text{CV}(\lambda_t)$ .

We used pairwise Pearson correlation tests to confirm that the relationships between these life history parameters corresponded to those expected from life history theory. We expected  $GT$  to increase with decreased  $E(M_{a,t})$  and  $\lambda_t$ , indicating a transition from the fast end to the slow end of the continuum among the species examined. We also expected the  $\text{Var}(M_{a,t})$  and  $\text{CV}(\lambda_t)$ , to increase with increasing  $E(M_{a,t})$  and  $\lambda_t$  respectively.

### Estimation of spatial scaling and population synchrony

The spatial scaling of population variables was estimated using data from scientific bottom trawl surveys performed annually by the Norwegian Institute for Marine Research and the Polar Research Institute of Marine Fisheries and Oceanography from January to March, from 1985 to 2016 (Jakobsen *et al.* 1997; Aanes & Vølstad 2015). The survey followed a stratified sampling design with approximately uniform distribution of sampled locations in space and was, with few exceptions, performed using Campelen 1800 demersal survey trawls with mesh sizes of 22 mm in the codend that were towed for  $\sim 30$  min at a speed of 3 knots and an effecting height of  $\sim 4$  m (3.5–5 m; Aglen 1996). The area covered by the trawls and the geometry of the trawls (i.e. door spread, mouth opening, relative velocity and contact with the bottom) were monitored with doppler logs or GPS and SCANMAR system respectively. For more details see: Jakobsen *et al.* (1997), Johannessen *et al.* (2009) and Pennington *et al.* (2011).

The survey data were used to estimate site-specific indices of abundance and yearly change in abundance. A site is defined as each of the cells of hexagonal grids placed over the study region. Yearly changes in abundance are defined as changes in local abundance from a given year to the next and are

expected to be driven by fish returning or remaining around the same regions after undergoing spawning migrations, and thereafter influenced by dispersal dynamics, density regulation and mortality rates. To assess the influence of the spatial resolution of the hexagonal grid on the spatial synchrony estimates, we estimated indices of abundance and yearly changes in abundance over cell sizes of 2 500, 4 900, 8 100, 12 100, 16 900, 22 500, 28 900, 36 100 (Fig. 1), 44 100 and 52 900 km<sup>2</sup>. The 36 100 km<sup>2</sup> resolution was chosen for this study based on a balance between minimising the number of incomplete series and reducing the risk of losing spatial signalling for all species included in this study. Results from the analysis using other resolutions are presented in the supplementary materials (Appendix S2). For simplicity, we performed the spatial analyses under the assumption that distance decay is isotropic. It is possible that underlying spatial heterogeneity could cause different rates of decay in different directions in some cases, but there is no reason to believe that this assumption would cause systematic biases.

Catch numbers divided by the area swept by the trawl were considered to be direct observations of density (cf. Aanes & Vølstad 2015), and local densities ( $N$ ) were estimated by averaging the sampled densities per cell area and year. Local changes in abundance at time  $t$  were defined as the log of the ratio of abundance in subsequent years, i.e.  $r_t = \log(N_{t+1}/N_t)$ . The resulting estimates of log abundance ( $\log(N_t)$ ) and the log of annual changes in abundance ( $r_t$ ) were compiled into time series for each grid-cell. Values of  $N_t$  that were 0 were omitted from the analysis as they will result in undefined values of both  $\log(N_t)$  and  $r_t$ , and hence all results are conditioned on  $N_t > 0$ .

Spatial autocorrelation in the variables  $\log(N)$  and  $r$  were each estimated with a model where the data are assumed spatially dependent but independent in time, following principles for introducing spatial dependence (see e.g. Cressie & Wikle 2011). For the variable of interest at site  $s$  and time  $t$ ,  $y(s, t)$ , we write

$$y(s, t) = \kappa(s) + W(s, t) + \varepsilon(s, t) \quad (1)$$

where  $\kappa(s)$  is the mean at site  $s$ ,  $W(s, t)$  is a spatially dependent and  $\varepsilon(s, t)$  a spatially independent, both zero mean, random variables. Then  $W(s, t)$  includes the spatially structured deviations from the mean and  $\varepsilon(s, t)$  the residual variability representing microscale and sampling variability. The covariance function of spatial distance  $d$  is defined as

$$C_W(d) = \text{Cov}(W(s, t), W(r, t)) = \sigma(s)\sigma(r)\rho_Y(d) \quad (2)$$

where  $\sigma(s)$  is the variance at site  $s$ ,  $\rho_Y(d) = [\rho_\infty + (\rho_0 - \rho_\infty)h(d)]$  is the spatial autocorrelation at distance  $d$ , where  $\rho_\infty$  and  $\rho_0$  are the correlations of the population variables at infinity and zero distance respectively. The spatial dependence is captured by  $h(d) = \exp\left(-\frac{d^2}{2l^2}\right)$ , which is a Gaussian function where the parameter  $l$  defines the spatial scaling. The residual variation is included in  $\varepsilon$  and is independent of  $W(s, t)$ , such that

$$\begin{aligned} C_Y(d) &= \text{Cov}(Y(s, t), Y(r, t)|\kappa(s), \kappa(r)) \\ &= \text{Cov}(W(s, t), W(r, t)) + \sigma_\varepsilon^2 I(d = 0) \end{aligned} \quad (3)$$

Assuming  $\sigma(s) = \sigma(r) = \sigma$ , that is, variance is equal across space, we get the covariance function

$$C_Y(d) = \sigma^2[\rho_\infty + (\rho_0 - \rho_\infty)h(d)] + \sigma_\epsilon^2 \mathbf{I}(d=0) \quad (4)$$

Writing  $\mathbf{Y}_t = (Y(s_1, t), Y(s_2, t), \dots, Y(s_{n_s}, t))'$ ,  $n_s$  being the number of sites, we have  $E(\mathbf{Y}_t|\kappa) = \kappa$  and  $\text{Var}(\mathbf{Y}_t|\kappa) = \Sigma + \sigma_\epsilon^2 \mathbf{I}$  where the elements in  $\Sigma$  are defined by  $\text{Cov}(W(s, t), W(r, t))$ . Assuming all  $W$  and  $\epsilon$  follow normal distributions, it may then be shown that the mean corrected values are approximately multivariate normally distributed

$$\mathbf{y}(t) - \hat{\kappa} \sim MVN(0, \Sigma + \sigma_\epsilon^2 \mathbf{I}) \quad (5)$$

where  $\hat{\kappa}$  is the vector of mean values at each location. Hence, the likelihood function  $L(\mathbf{y}(t) - \hat{\kappa}; \theta) = \prod_{t=1}^T f(\mathbf{y}(t) - \hat{\kappa}|\theta)$  is completely specified, such that the parameters  $\rho_0$ ,  $\rho_\infty$ ,  $\sigma^2$  and  $l$  can be estimated by numerical optimisation. Distributions of parameters are obtained by non-parametric bootstrapping achieved by resampling vectors of annual  $\mathbf{Y}_t$  with replacement and subsequently fitting the model to each replicate dataset.

Generalised linear models (GLMs) were used to analyse the relationship between each life history trait and scaling of synchrony (i.e.  $l$  in the Gaussian function,  $h(d)$ ) of abundance and yearly changes in abundance, independently. Estimates of spatial scaling were log-transformed to linearise their relationship with the life history parameters. First, we used GLMs of the form  $\log(Z) = \beta_0 + \beta_1 X$ , where the response variable,  $Z$ , is the spatial scaling parameters  $l_{\log(N)}$  or  $l$ ,  $\beta_0$  is the intercept of the model,  $X$  represents one of the life history parameters ( $GT$ ,  $E(M_{a,t})$ ,  $\text{Var}(M_{a,t})$ ,  $\lambda_t$  or  $\text{CV}(\lambda_t)$ ) and  $\beta_1$  represents the rate at which the spatial scaling changes in response to unit changes in the life history traits. The spatial scaling parameter was represented by the median of the distribution of synchrony scalings obtained through a bootstrapping. To account for the heteroskedasticity and non-normality of the variables, we bootstrap-resampled the model 50 000 times using random

values from each of the models' variables. This resulted in 50 000 slope and intercept estimates for each of the ten models. Lastly, to examine the presence of a general relationship between spatial scaling and life history traits, we measured the proportion of positive or negative slopes within the resulting model outputs. All data analyses were carried out in R version 3.5.0 (R Core Team 2018).

## RESULTS

### Life history strategies

As expected, generation times,  $GT$ , were negatively correlated with expected natural mortality rates at age and year,  $E(M_{a,t})$  (Pearson's  $r$  ( $R_p$ ) =  $-0.89$ ,  $n = 8$ ,  $P = 0.003$ ), and with annual multiplicative population growth rates,  $\lambda_t$  ( $R_p = -0.85$ ,  $n = 8$ ,  $P = 0.007$ ). Correspondingly,  $E(M_{a,t})$  and  $\lambda_t$  were positively correlated ( $R_p = 0.89$ ,  $n = 8$ ,  $P = 0.003$ ). In this study, capelin, blue whiting and haddock represented the faster end of the continuum, while beaked redfish and golden redfish represented the slow end (Table 1).

The CV of population growth rate,  $\text{CV}(\lambda_t)$ , were positively correlated with  $\lambda_t$  ( $R_p = 0.94$ ,  $n = 8$ ,  $P < 0.001$ ), but negatively with  $GT$  ( $R_p = -0.74$ ,  $n = 8$ ,  $P = 0.037$ ). On the other hand, variance in mortality,  $\text{Var}(M_{a,t})$ , was not significantly correlated with  $E(M_{a,t})$  ( $R_p = 0.64$ ,  $n = 8$ ,  $P = 0.089$ ), nor with  $GT$  ( $R_p = -0.56$ ,  $n = 8$ ,  $P = 0.145$ ).

### Spatial scaling of abundance and yearly change in abundance

The scaling estimates of abundance varied markedly among species, more than doubling in distance from the shortest (capelin and haddock) to the longest (golden redfish; Table 1).

**Table 1** Estimated spatial scaling ( $l$ ) of abundance ( $\log(N)$ ) and annual change in abundance ( $r$ ) with corresponding 95% confidence intervals in brackets, as well as the estimated values for each life history trait obtained from Bjørkvoll *et al.* (2012) with their 95% credible intervals

Species	$l$ (km)		$r$
	$l$	$\log(N)$	
Golden redfish	501.8 (317.2, 803.2)		352.2 (7.5, 569.5)
Beaked redfish	363.0 (124.0, 613.4)		141.3 (103.2, 375.4)
NSS herring	247.3 (181.0, 320.6)		221.7 (6.6, 355.4)
NEA saithe	306.3 (84.9, 504.6)		30.7 (3.7, 212.01)
NEA cod	279.4 (144.4, 414.5)		375.1 (202.7, 496.2)
NEA haddock	198.7 (138.0, 308.8)		270.4 (132.9, 426.5)
Blue whiting	218.7 (165.1, 343.5)		391.4 (212.8, 573.9)
Barents Sea capelin	201.7 (139.0, 273.3)		118.5 (12.1, 205.5)

Species	Population parameteres estimates from				
	$GT$	$\lambda_t$	$\text{CV}(\lambda_t)$	$E(M_{a,t})$	$\text{Var}(M_{a,t})$
Golden redfish	14.686 (14.233, 15.143)	0.974 (0.958, 0.989)	0.026 (0.017, 0.043)	0.031 (0.007, 0.079)	0.001 (0.000, 0.003)
Beaked redfish	14.273 (13.975, 14.499)	1.032 (1.009, 1.054)	0.154 (0.114, 0.250)	0.065 (0.010, 0.149)	0.005 (0.000, 0.030)
NSS herring	6.793 (6.438, 7.161)	1.138 (1.093, 1.201)	0.290 (0.175, 0.448)	0.254 (0.150, 0.388)	0.270 (0.035, 1.204)
NEA saithe	6.652 (6.291, 7.072)	1.106 (1.056, 1.169)	0.235 (0.144, 0.394)	0.244 (0.067, 0.447)	0.027 (0.001, 0.111)
NEA cod	6.592 (6.39, 6.737)	1.212 (1.163, 1.259)	0.342 (0.232, 0.495)	0.336 (0.153, 0.578)	0.042 (0.010, 0.103)
NEA haddock	5.757 (5.447, 6.05)	1.332 (1.260, 1.411)	0.560 (0.434, 0.725)	0.424 (0.243, 0.640)	0.109 (0.036, 0.287)
Blue whiting	4.110 (3.920, 4.283)	1.346 (1.250, 1.438)	0.307 (0.214, 0.462)	0.250 (0.051, 0.485)	0.034 (0.001, 0.122)
Barents Sea capelin	2.644 (2.312, 3.050)	1.597 (1.267, 2.241)	1.033 (0.643, 1.841)	0.508 (0.034, 1.204)	0.273 (0.000, 1.362)

Increasing the cell sizes of the grid used to calculate spatial synchrony generally increased the estimated spatial scaling of abundance for all species. Coarser resolutions also reduced the uncertainty of the estimates for species with less spatial data that showed high uncertainty at finer resolutions, for example, Saithe (Appendix S2). We present the results from the analysis performed at a resolution of 36 100 km<sup>2</sup>. This resolution represents a good balance between fine spatial resolution and minimising noise/error in the abundance estimates. Scaling estimates of yearly changes in abundance differed inconsistently from the scaling estimates of abundance, being in some cases greater and in other cases shorter for different species (Table 1). Varying the resolution influenced the scaling estimates in an inconsistent matter, although coarser resolution generally reduced the overall uncertainty of the estimate (Appendix S2).

### Life history strategy and spatial scaling

We found a higher spatial scaling of abundance (i.e. synchrony over larger distances,  $l_{\log(N)}$ ) in species with slower life

histories. This trend was consistent across the resolutions used in the spatial synchrony analysis. Uncertainty in the estimated relationship decreased with coarser resolutions (Appendix S2). No significant correlation was found between the spatial scaling of yearly change in abundance,  $l_r$ , and life history strategy regardless of the spatial resolutions examined.

We found a positive relationship between species' generation time,  $GT$ , and  $l_{\log(N)}$  ( $\beta_{GT,N} = 0.066$ , 95% CI = (0.041, 0.090),  $P = 0.002$ ; Fig. 2a). The positive relationship was persistent when accounting for the variance within both variables, as 98.7% of the slopes from the bootstrap was positive. Increasing population growth,  $\lambda_t$ , predicted a decline in  $l_{\log(N)}$  ( $\beta_{\lambda_t,N} = -1.351$ , 95% CI = (-2.011, -0.689),  $P = 0.007$ ), also evident when accounting for the uncertainty in the variables as 98.7% of the slopes supported a negative correlation (Fig. 2b). A negative pattern was also present in the relationship between  $CV(\lambda_t)$  and  $l_{\log(N)}$  ( $\beta_{CV(\lambda_t),N} = -0.786$ , 95% CI = (-1.324, -0.247),  $P = 0.029$ ), where 98.6% of the bootstrapped models predicted a negative relationship (Fig. 2c). Expected mortality rate,  $E(M_{a,t})$ , showed significant negative correlation with  $l_{\log(N)}$  ( $\beta_{E(M),N} = -1.770$ , 95%

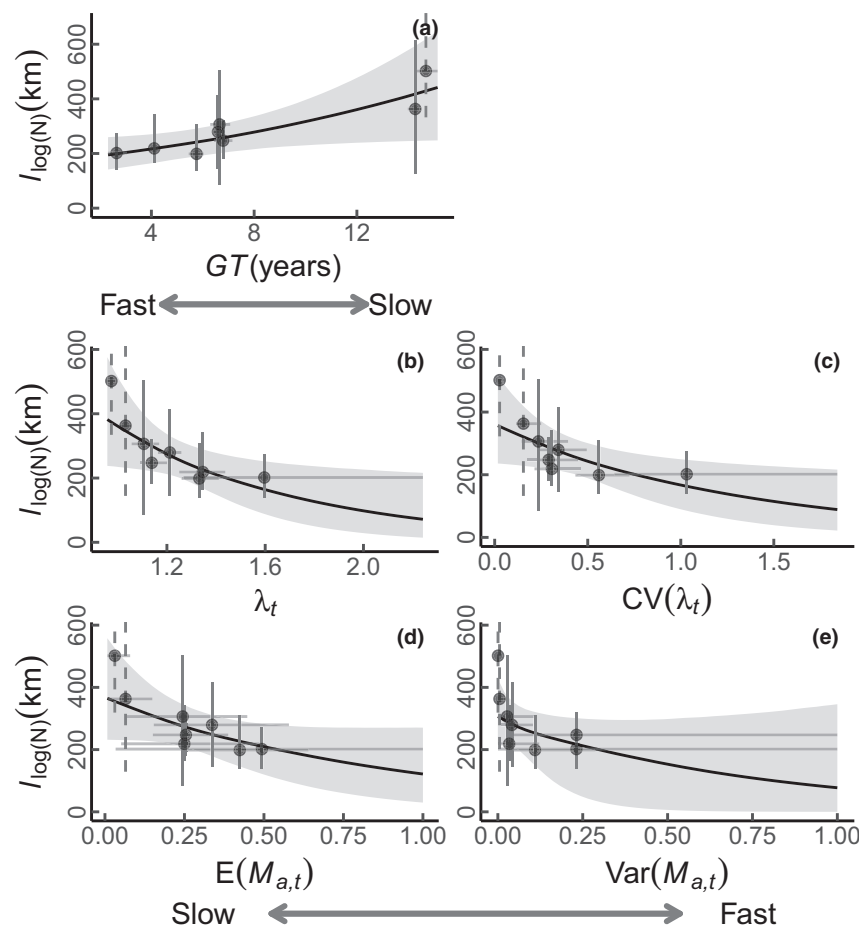


**Figure 2** Relationship between spatial scaling of abundance,  $l_{\log(N)}$ , and (a) generation time,  $GT$ , (b) multiplicative population growth rate,  $\lambda_t$ , (c)  $CV$  of the multiplicative population growth rate,  $CV(\lambda_t)$ , (d) expected mortality rate,  $E(M_{a,t})$  and (e) variance of mortality,  $Var(M_{a,t})$ . Points represent the median of each species' spatial scaling estimates and their estimated life history traits, with the vertical and horizontal lines indicate their 95% confidence intervals and credible intervals respectively. The dashed lines should reach (from left to right) 803 and 613 km, but the range of the y-axis was delimited. The regression line shows the model's prediction with the uncertainty shown by the 95% credible sets in grey. The arrow under the x axis indicates the direction of the relationship between the life history traits and the slow-fast continuum.

$\text{CI} = (-2.520, -1.012)$ ,  $P = 0.003$ ), with 97% of the bootstrapped models supporting the relationship (Fig. 2d). The relationship between the species' average estimated  $\text{Var}(M_{a,t})$  and the median of their estimated  $l_{\log(N)}$  values showed a negative trend as well, although non-significant ( $\beta_{\text{Var}(M,N)} = -2.11$ , 95% CI =  $(-4.162, -0.064)$ ,  $P = 0.090$ ). The bootstrap-resampling of the model indicated that 94.1% of the models between  $\text{Var}(M_{a,t})$  and  $l_{\log(N)}$  instances supported a negative relationship (Fig. 2e).

The  $GT$  of a species was not found to be correlated with  $l_r$  ( $\beta_{GT,r} = 0.02$ , 95% CI =  $(-0.136, 0.172)$ ,  $P = 0.826$ ), even when accounting for the variance within both variables in the bootstrap approach ( $P(\beta_1 < 0 = 0.48)$ ; Fig. 3a). Likewise,  $l_r$  was not found to be dependent on  $\lambda_t$  ( $\beta_{\lambda,r} = 0.164$ , 95% CI =  $(-3.232, 3.559)$ ,  $P = 0.928$ ;  $P(\beta_1 < 0 = 0.483)$ ; Fig. 3b), nor dependent on the population's  $\text{CV}(\lambda_t)$  ( $\beta_{\text{CV}(\lambda),r} = -0.798$ , 95% CI =  $(-2.414, 4.009)$ ,  $P = 0.644$ ;  $P(\beta_1 < 0 = 0.484)$ ; Fig. 3c). Finally, neither  $E(M_{a,t})$  nor  $\text{Var}(M_{a,t})$  were found to be predictors of variation in  $l_r$  ( $\beta_{E(M),r} = -0.356$ , 95% CI =  $(-4.647, 3.934)$ ,  $P = 0.876$ ;  $P(\beta_1 < 0 = 0.59)$ ;  $\beta_{\text{Var}(M,r)} = -0.4214$ , 95% CI =  $(-7.534, 6.691)$ ,  $P = 0.911$ ;  $P(\beta_1 < 0 = 0.54)$ ; Fig. 3d-e).

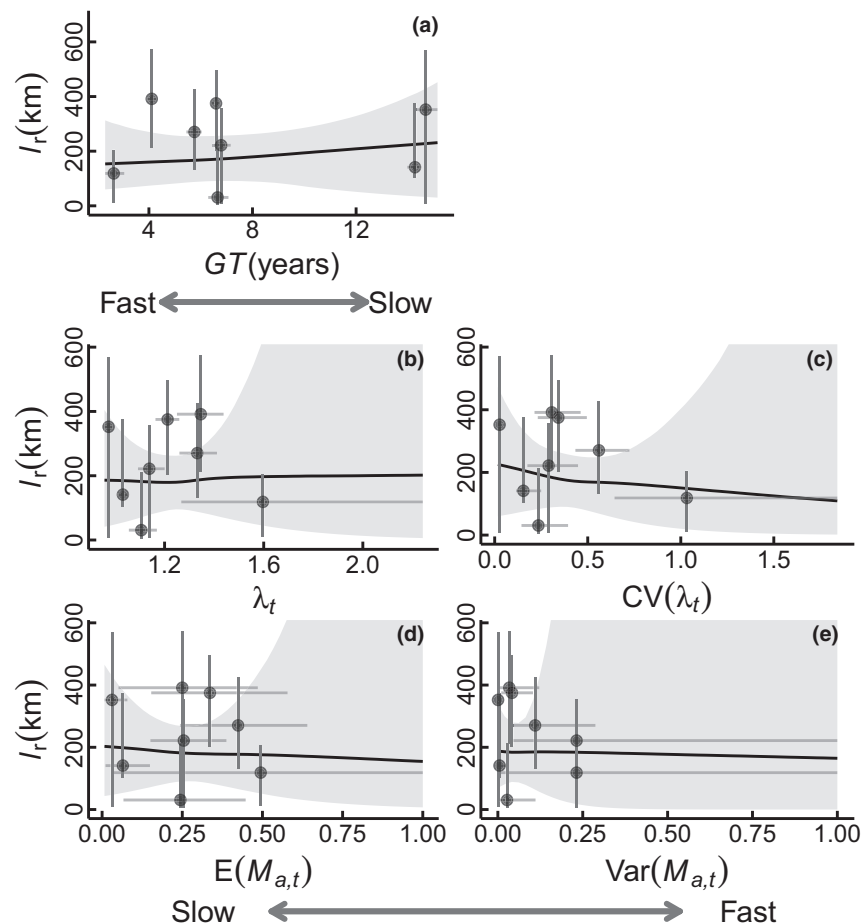


**Figure 3** Relationship between spatial scaling of annual changes in abundance,  $l_r$ , and (a) generation time,  $GT$ , (b) multiplicative population growth rate,  $\lambda_t$ , (c)  $\text{CV}$  of the multiplicative population growth rate,  $\text{CV}(\lambda_t)$ , (d) expected mortality rate,  $E(M_{a,t})$  and (e) variance of mortality,  $\text{Var}(M_{a,t})$ . Points represent the median of each species' spatial scaling estimates and their estimated life history traits, with the vertical and horizontal lines indicate their 95% confidence intervals and credible intervals respectively. The regression line shows the model's prediction with the uncertainty shown by the 95% credible sets in grey. The arrow under the x axis indicates the direction of the relationship between the life history traits and the slow-fast continuum.

## DISCUSSION

Our results show that among species variation in the spatial scaling of abundance synchrony is related to life history in a way that follows the slow-fast continuum, where species located at the slow end have greater spatial scaling of abundance. The general relationship between spatial scaling of abundance and life history was robust to variation in the resolution used to calculate spatial synchrony, at least within the resolution margins explored here. Scaling of synchrony in annual change in abundance also varied with resolution, but was not found to depend on life history parameters under any of the resolutions analysed. Our findings highlight an important connection between species life histories and spatial population dynamics and suggest that knowledge of a species' life history could give an indication of its expected spatial distribution and synchrony, at least among marine fish species.

The slow-fast continuum is a useful predictor of life history variation in a range of taxa, including birds (Sæther & Bakke 2000), mammals (Oli 2004; van de Kerk *et al.* 2013) and reptiles (Shine & Charnov 1992; Clobert *et al.* 1998). While

previous studies have identified a trilateral continuum model with up to five distinct life history strategies among fish species (Winemiller & Rose 1992; King & McFarlane 2003), Bjørkvoll *et al.* (2012) showed how a simple linear continuum could describe life history variation in fish species from the Barents Sea community. Towards the slow end species had low reproduction and mortality, slow population growth and long generation times, while fast-lived species showed contrasting attributes. Our results showed the same pattern, despite our smaller species sample size and a different methodology. Furthermore, our findings expand our understanding of life history covariation patterns by showing that the spatial scale of synchrony in abundance within a population correlates with the slow-fast continuum.

Although the main factors causing spatial synchrony (i.e. dispersal, environmental forcing and trophic interactions) are well documented across taxa (e.g. Hanski & Woiwod 1993; Koenig 2001; Grøtan *et al.* 2005; Frank *et al.* 2016), little is known about how a species' pace of life influences these factors. Theoretical studies have proposed mechanisms to link spatial scaling to species traits in ways that are consistent with the general pattern shown empirically here. Lande *et al.* (1999) showed with the general formula  $I_p^2 = I_e^2 + ml^2/\gamma$  that a population's spatial scale of synchrony in abundance ( $I_p^2$ ) depends on the spatial scale of environmental synchrony ( $I_e^2$ ), individual dispersal rate ( $m$ ), and dispersal distance ( $l^2$ ), but that the contribution of dispersal could be regulated by the strength of density regulation ( $\gamma$ ), which is correlated with pace of life (Beddington & May 1977; Herrando-Pérez *et al.* 2012). This idea was further developed to allow for higher environmental noise (Engen 2017), showing that individuals from species with lower population growth rates or weaker density regulated populations, such as those towards the slow end of the slow-fast continuum, are expected to disperse farther, allowing them to contribute significantly more to synchrony over larger distances. Other simulation studies have also shown that slower population growth rate and lower reproductive rates increased the relative contribution of dispersal to synchrony, allowing synchrony in population dynamics to extend beyond the one generated by the environment (Söndgerath & Schröder 2002; Ranta *et al.* 2006; Bahn *et al.* 2008). Given the known associations that traits like density regulation, reproductive rate or growth rate have within the slow fast continuum (Herrando-Pérez *et al.* 2012), it makes sense that a pattern of covariation between the pace of life and spatial scaling exists.

Results from previous studies on wild populations that included both measurements of spatial population dynamics and of a life history trait provide some support to the reported pattern. Without making reference to spatial autocorrelation, Kuo *et al.* (2016) showed that slower lived fish species tended to be more homogeneously distributed in space compared to fast lived ones, and hypothesised that greater resistance to stochastic events of slow lived species may be responsible for the pattern (Johst & Brandl 1997). Similarly, a study on British bird populations found that larger body size correlated positively but not significantly with the rate of synchrony decline with increased distance (Paradis *et al.* 2000), supporting our general pattern. However, when they removed

the variation caused by changes in the global population abundance to assess how local factors alone were driving synchrony, the correlation between the variables was negative.

Spatial scaling in the synchrony of annual changes in abundance was not found to be predicted by life history. This could be influenced by several factors, but movement dynamics is likely to be a major driver. Homing behaviour could be affecting the spatial synchrony of changes in abundance (Östman *et al.* 2017), and is also a population characteristic that is not associated with life history. For example, all species studied here migrate annually to spawning grounds and feeding grounds (Olsen *et al.* 2010). While the feeding grounds of some of the species studies might be spatially stable (e.g. haddock, cod), other species have more variable feeding grounds. Capelin tends to move northward to follow the plankton blooms triggered by the melting of the sea ice. However, as the melting rate of the ice varies among years (Fosseim *et al.* 2015), the spatial distribution of capelin will also vary, decoupling the abundance at a given site between subsequent years. In addition, many of the species included in our study tend to be age-segregated in space (Olsen *et al.* 2010). Changes in the age structure of the population, induced by for example harvesting, might therefore cause decreased synchrony among local annual changes in abundance (Kuo *et al.* 2016).

The choice of spatial resolution in the grouping of the data can have significant effects on the resulting patterns (Pearson & Carroll 1999; Dungan *et al.* 2002). Here, the choice of resolution in the spatial synchrony analyses influenced the resulting scaling estimates differently depending on the species, but not the relationship between scaling and life history. In fact, the relationship became clearer with coarser resolution. This phenomenon is known as the 'modifiable areal unit problem' (Liebhold *et al.* 2012). Variation in the amount of data available for some species, as well as the omission of zeros during the analyses probably led to greater variation at finer resolutions, which was improved after reaching certain resolutions for each of the species. Moreover, increasing the resolution tended to result in higher estimates of scaling for all species, while the uncertainty in the estimates for some species decreased greatly (e.g. saithe).

The observed extents of the spatial scaling of synchrony in abundance and its annual variation are comparable to previous studies on fish (Myers *et al.* 1997; Östman *et al.* 2017), and indicate that widely synchronised environmental forces and/or dispersal are acting on the populations (Grenfell *et al.* 1998). Interspecific variation in the intensity of external factors, like harvesting pressure, is also expected to cause variation in synchrony (Frank *et al.* 2016) by for example altering the age/size structure of populations (Jørgensen & Holt 2013; Kuo *et al.* 2016). Homing behaviours or diet preferences could also influence the dispersal patterns of the species studied differently affecting their synchrony, where food generalists might not need to search as much as specialists, thereby decreasing their dispersal (Yaragina & Dolgov 2009).

All the data used in this study were collected by bottom-trawl surveys. It could be argued that bottom trawling is less appropriate for the two pelagic species in our study (capelin and herring) than for the demersal species (McQuinn 2009; Frank *et al.* 2013). However, bottom trawls can be used to monitor the

abundance of pelagic species under the assumption that a constant fraction of the population is available in the sampling volume of the trawl (near the bottom) between years. Pelagic fish species, like herring, are often found near the bottom in shelf areas like the Barents Sea and the North Sea. Therefore, bottom trawl surveys have been used in the stock assessments of for example North Sea herring (see e.g. ICES 2018).

Our results have important implications under future climate change scenarios. Recent publications have predicted that climate change and associated ecological processes (e.g. increased competition or predation) will change population life histories and spatial distributions (Swain *et al.* 2015; Pinneel *et al.* 2016; Lancaster *et al.* 2017). In addition, climate change and other anthropogenic disturbances that alter population cycles, such as harvesting, have been shown to influence the spatial synchrony of populations, with uncertain consequences for their future (Bjørnstad 2000; Vasseur & Fox 2009; Defriez *et al.* 2016; Shestakova *et al.* 2016). Understanding the link between the two processes, and what additional factors could influence spatial synchrony (e.g. geography of synchrony, (Walter *et al.* 2017)), should be a priority within spatial ecology. Although the current study shows quite a clear pattern between life history and spatial scaling of abundance it is based on a limited number of species. It will therefore be important to follow this up with further empirical studies of this pattern, both in the marine environment and among a variety of taxa and ecosystems.

Despite there not being a single mechanism able to explain spatial patterns across scales (Levin 1992), we present a robust pattern that describes how spatial synchrony in population dynamics varies with distance based on the species' pace of life. This relationship helps to bridge knowledge gaps associated with spatial scaling to life history, thereby facilitating a better understanding of population dynamics and potential vulnerabilities associated to their spatial distributions. We encourage the testing of this pattern in other species groups to clarify its generality across ecosystems. Given current ecological challenges, like habitat fragmentation, climate driven invasions or disease outbreaks, the presented pattern could provide important guidelines for future harvesting and conservation strategies.

## ACKNOWLEDGEMENTS

We are grateful to Eirin Bjørkvoll for facilitating access to the raw results of her paper and providing assistance in their use. In addition, J.F.M. thanks Stefan Vriend for all the support and advice. Lastly, we are grateful to James Thorson and two anonymous referees for providing valuable comments in an early version of the paper that we included into the final work. This study was funded by the Research Council of Norway through the Centre of Excellence (project 223257) and research project SUSTAIN (244647).

## AUTHORSHIP

BES, SE, IH, SA and AML planned the study. SA and AS collated the data. SA performed the spatial scaling analyses. JFM performed all other statistical analyses with input from

SA and AML. JFM wrote the manuscript with contributions from all other authors.

## DATA AVAILABILITY STATEMENT

The life history data is available in Bjørkvoll *et al.* (2012), while all the data used in the spatial analyses will be made available from the Figshare Repository: <https://doi.org/10.6084/m9.figshare.8427212>.

## REFERENCES

- Aanes, S. & Vølstad, J.H. (2015). Efficient statistical estimators and sampling strategies for estimating the age composition of fish. *Can. J. Fish. Aquat. Sci.*, 72, 938–953.
- Aanes, S., Engen, S., Sæther, B.-E. & Aanes, R. (2007). Estimation of the parameters of fish stock dynamics from catch-at-age data and indices of abundance: can natural and fishing mortality be separated? *Can. J. Fish. Aquat. Sci.*, 64, 1130–1142.
- Aglen, A. (1996). Impact of fish distribution and species composition on the relationship between acoustic and swept-area estimates of fish density. *ICES J. Mar. Sci.*, 53, 501–505.
- Bahn, V., Krohn, W.B. & O'Connor, R.J. (2008). Dispersal leads to spatial autocorrelation in species distributions: a simulation model. *Ecol. Modell.*, 213, 285–292.
- Barraquand, F. & Murrell, D.J. (2012). Intense or spatially heterogeneous predation can select against prey dispersal. *PLoS ONE*, 7, e28924.
- Beddington, J.R. & May, R.M. (1977). Harvesting natural populations in a randomly fluctuating environment. *Science (80-)*, 197, 463–465.
- Bjørkvoll, E., Grøtan, V., Aanes, S., Sæther, B.-E., Engen, S. & Aanes, R. (2012). Stochastic population dynamics and life-history variation in marine fish species. *Am. Nat.*, 180, 372–387.
- Bjørnstad, O.N. (2000). Cycles and synchrony: two historical ‘experiments’ and one experience. *J. Anim. Ecol.*, 69, 869–873.
- Bjørnstad, O.N. & Bolker, B. (2000). Canonical functions for dispersal-induced synchrony. *Proc. R. Soc. B Biol. Sci.*, 267, 1787–1794.
- Bjørnstad, O.N., Ims, R.A. & Lambin, X. (1999). Spatial population dynamics: analyzing patterns and processes of population synchrony. *Trends Ecol. Evol.*, 14, 427–432.
- Clobert, J., Garland, T. Jr & Barbault, R. (1998). The evolution of demographic tactics in lizards: a test of some hypotheses concerning life history evolution. *J. Evol. Biol.*, 11, 329–364.
- Cressie, N. & Wikle, C.K. (2011). *Statistics for Spatio-temporal Data*. John Wiley & Sons, Hoboken, NJ.
- Defriez, E.J., Sheppard, L.W., Reid, P.C. & Reuman, D.C. (2016). Climate change-related regime shifts have altered spatial synchrony of plankton dynamics in the North Sea. *Glob. Chang. Biol.*, 22, 2069–2080.
- Dungan, J.L., Perry, J.N., Dale, M.R.T., Legendre, P., Citron-Pousty, S., Fortin, M.J. *et al.* (2002). A balanced view of scale in spatial statistical analysis. *Ecography (Cop.)*, 25, 626–640.
- Ellis, J. & Schneider, D.C. (2008). Spatial and temporal scaling in benthic ecology. *J. Exp. Mar. Bio. Ecol.*, 366, 92–98.
- Engen, S. (2007). Stochastic growth and extinction in a spatial geometric Brownian population model with migration and correlated noise. *Math. Biosci.*, 209, 240–255.
- Engen, S. (2017). Spatial synchrony and harvesting in fluctuating populations: relaxing the small noise assumption. *Theor. Popul. Biol.*, 116, 18–26.
- Engen, S., Lande, R. & Sæther, B. (2002). The spatial scale of population fluctuations and quasi-extinction risk. *Am. Nat.*, 160, 439–451.
- Engen, S., Lande, R., Sæther, B.-E. & Weimerskirch, H. (2005a). Extinction in relation to demographic and environmental stochasticity in age-structured models. *Math. Biosci.*, 195, 210–227.

- Engen, S., Lande, R., Sæther, B.E. & Bregnballe, T. (2005b). Estimating the pattern of synchrony in fluctuating populations. *J. Anim. Ecol.*, 74, 601–611.
- Engen, S., Cao, F.J. & Sæther, B. (2018). The effect of harvesting on the spatial synchrony of population fluctuations. *Theor. Popul. Biol.*, 123, 28–34.
- Fauchald, P., Mauritzen, M. & Gjøsæter, H. (2006). Density-dependent migratory waves in the marine pelagic ecosystem. *Ecology*, 87, 2915–2924.
- Ferguson, S.H. & Larivière, S. (2002). Can comparing life histories help conserve carnivores? *Anim. Conserv.*, 5, 1–12.
- Fosseheim, M., Primicerio, R., Johannessen, E., Ingvaldsen, R.B., Aschan, M.M. & Dolgov, A.V. (2015). Recent warming leads to a rapid borealization of fish communities in the Arctic. *Nat. Clim. Chang.*, 5, 673–677.
- Frank, K.T., Leggett, W.C., Petrie, B.D., Fisher, J.A.D., Shackell, N.L. & Taggart, C.T. (2013). Irruptive prey dynamics following the groundfish collapse in the Northwest Atlantic: an illusion? *ICES J. Mar. Sci.*, 70, 1299–1307.
- Frank, K.T., Petrie, B., Leggett, W.C. & Boyce, D.G. (2016). Large scale, synchronous variability of marine fish populations driven by commercial exploitation. *Proc. Natl Acad. Sci.*, 113, 8248–8253.
- Giometto, A., Altermatt, F. & Rinaldo, A. (2017). Demographic stochasticity and resource autocorrelation control biological invasions in heterogeneous landscapes. *Oikos*, 126, 1554–1563.
- Grenfell, B.T., Wilson, K., Finkenstädt, B.F., Coulson, T.N., Murray, S., Albon, S.D. et al. (1998). Noise and determinism in synchronized sheep dynamics. *Nature*, 394, 674–677.
- Grøtan, V., Sæther, B.-E., Engen, S., Solberg, E.J., Linnell, J.D., Andersen, R. et al. (2005). Climate causes large-scale spatial synchrony in population fluctuations of a temperature herbivore. *Ecology*, 86, 1472–1482.
- Hanski, I. & Woiwod, I.P. (1993). Spatial synchrony in the dynamics of moth and aphid populations. *J. Anim. Ecol.*, 62, 656.
- Heino, M., Kaitala, V., Ranta, E. & Lindström, J. (1997). Synchronous dynamics and rates of extinction in spatially structured populations. *Proc. R. Soc. London B Biol. Sci.*, 264, 481–486.
- Herrando-Pérez, S., Delean, S., Brook, B.W. & Bradshaw, C.J.A. (2012). Strength of density feedback in census data increases from slow to fast life histories. *Ecol. Evol.*, 2, 1922–1934.
- Huse, G. (2016). A spatial approach to understanding herring population dynamics. *Can. J. Fish. Aquat. Sci.*, 73, 177–188.
- ICES (2008a). Report of the Arctic Fisheries Working Group (AFWG). Copenhagen, Denmark.
- ICES (2008b). Report of the Working Group on Widely Distributed Stocks (WGWHITE). Copenhagen, Denmark.
- ICES (2009). Report of the Arctic Fisheries Working Group (AFWG). San Sebastian, Spain.
- ICES (2016). Ecosystem overviews: Barents Sea Ecoregion. ICES Advice 2016, B, 9, 8.
- ICES (2018). Report of the Herring Assessment Working Group for the Area South of 62°N (HAWG). ICES HQ, Copenhagen, Denmark.
- Ims, R.A. & Andreassen, H.P. (2000). Spatial synchronization of vole population dynamics by predatory birds. *Nature*, 408, 194–196.
- Jakobsen, T., Korsbække, K., Mehl, S. & Nakken, O. (1997). Norwegian combined acoustic and bottom trawl surveys for demersal fish in the Barents Sea during winter. *ICES J. Mar.*, 17, 26.
- Jennings, S., Reynolds, J.D. & Mills, S.C. (1998). Life history correlates of responses to fisheries exploitation. *Proc. R. Soc.*, 265, 333–339.
- Johannessen, E., Wenneck, T.D.L., Høines, Å., Aglen, A., Mehl, S., Mjanger, H. et al. (2009). Egner vinterstoktet seg til overvåking av endringer i fiskesamfunnet i Barentshavet: en gjennomgang av metodikk og data fra, 1981–2007, 29.
- Johst, K. & Brandl, R. (1997). Body size and extinction risk in a stochastic environment. *Oikos*, 78, 612.
- Jones, J., Doran, P.J. & Holmes, R.T. (2007). Spatial scaling of avian population dynamics: Population abundance, growth rate, and variability. *Ecology*, 88, 2505–2515.
- Jones, O.R., Gaillard, J.M., Tuljapurkar, S., Alho, J.S., Armitage, K.B., Becker, P.H. et al. (2008). Senescence rates are determined by ranking on the fast-slow life-history continuum. *Ecol. Lett.*, 11, 664–673.
- Jørgensen, C. & Holt, R.E. (2013). Natural mortality: Its ecology, how it shapes fish life histories, and why it may be increased by fishing. *J. Sea Res.*, 75, 8–18.
- Kausrud, K.L., Viljugrein, H., Frigessi, A., Begon, M., Davis, S., Leirs, H. et al. (2007). Climatically driven synchrony of gerbil populations allows large-scale plague outbreaks. *Proc. R. Soc. B Biol. Sci.*, 274, 1963–1969.
- Kendall, B.E., Bjørnstad, O.N., Bascompte, J., Keitt, T.H. & Fagan, W.F. (2000). Dispersal, environmental correlation, and spatial synchrony in population dynamics. *Am. Nat.*, 155, 628–636.
- van de Kerk, M., de Kroon, H., Conde, D.A. & Jongejans, E. (2013). Carnivora population dynamics are as slow and as fast as those of other mammals: Implications for their conservation. *PLoS ONE*, 8, e70354.
- King, J.R. & McFarlane, G.A. (2003). Marine fish life history strategies: applications to fishery management. *Fish. Manag. Ecol.*, 10, 249–264.
- Koenig, W.D. (1999). Spatial autocorrelation of ecological phenomena. *Trends Ecol. Evol.*, 14, 22–26.
- Koenig, W.D. (2001). Spatial autocorrelation and local disappearances in winter north american birds. *Ecology*, 82, 2636–2644.
- Kuo, T.C., Mandal, S., Yamauchi, A. & Hsieh, C.H. (2016). Life history traits and exploitation affect the spatial mean-variance relationship in fish abundance. *Ecology*, 97, 1251–1259.
- Lancaster, L.T., Morrison, G. & Fitt, R.N. (2017). Life history trade-offs, the intensity of competition, and coexistence in novel and evolving communities under climate change. *Philos. Trans. R. Soc. B Biol. Sci.*, 372(1712), 20160046.
- Lande, R., Engen, S. & Sæther, B.-E. (1999). Spatial scale of population synchrony: environmental correlation versus dispersal and density regulation. *Am. Nat.*, 154, 271–281.
- Levin, S.A. (1992). The problem of pattern and scale in ecology. *Ecology*, 73, 1943–1967.
- Liebold, A., Koenig, W.D. & Bjørnstad, O.N. (2004). Spatial synchrony in population dynamics. *Annu. Rev. Ecol. Syst.*, 35, 467–490.
- Liebold, A.M., Haynes, K.J. & Bjørnstad, O.N. (2012). Spatial synchrony of insect outbreaks. In: (eds. P. Barboda, D. K. Letourneau & A. A. Agrawal), *Insect Outbreaks Revisited*. John Wiley & Sons Ltd, Chichester, UK, pp. 113–125.
- Lindström, J., Ranta, E. & Lindén, H. (1996). Large-scale synchrony in the dynamics of capercaillie, black grouse and hazel grouse populations in Finland. *Oikos*, 76, 221–227.
- McQuinn, I.H. (2009). Pelagic fish outburst or suprabenthic habitat occupation: legacy of the Atlantic cod (*Gadus morhua*) collapse in eastern Canada. *Can. J. Fish. Aquat. Sci.*, 66, 2256–2262.
- Moran, P. (1953). The statistical analysis of the Canadian lynx cycle. II. Synchronization and meteorology. *Aust. J. Zool.*, 1, 291–298.
- Murdoch, W.W., Briggs, C.J., Nisbet, R.M. & Stewart-Oaten, A. (1992). Aggregation and stability in metapopulation models. *Am. Nat.*, 140, 41–58.
- Myers, R.A., Mertz, G. & Bridson, J. (1997). Spatial scales of interannual recruitment variations of marine, anadromous, and freshwater fish. *Can. J. Fish. Aquat. Sci.*, 54, 1400–1407.
- Oli, M.K. (2004). The fast–slow continuum and mammalian life-history patterns: an empirical evaluation. *Basic Appl. Ecol.*, 5, 449–463.
- Olsen, E., Aanes, S., Mehl, S., Holst, J.C., Aglen, A. & Gjøsæter, H. (2010). Cod, haddock, saithe, herring, and capelin in the Barents Sea and adjacent waters: a review of the biological value of the area. *ICES J. Mar. Sci.*, 67, 87–101.
- Östman, Ö., Olsson, J., Dannewitz, J., Palm, S. & Florin, A.B. (2017). Inferring spatial structure from population genetics and spatial synchrony in demography of Baltic Sea fishes: implications for management. *Fish Fish.*, 18, 324–339.
- Ovaskainen, O. & Cornell, S.J. (2006). Space and stochasticity in population dynamics. *Proc. Natl Acad. Sci.*, 103, 12781–12786.

- Paradis, E., Baillie, S.R., Sutherland, W.J. & Gregory, R.D. (1999). Dispersal and spatial scale affect synchrony in spatial population dynamics. *Ecol. Lett.*, 2, 114–120.
- Paradis, E., Baillie, S.R., Sutherland, W.J. & Gregory, R.D. (2000). Spatial synchrony in populations of birds: effects of habitat, population trend, and spatial scale. *Ecology*, 81, 2112.
- Pearson, D.L. & Carroll, S.S. (1999). The influence of spatial scale on cross-taxon congruence patterns and prediction accuracy of species richness. *J. Biogeogr.*, 26, 1079–1090.
- Pennington, M., Shevelev, M.S., Vølstad, J.H., Nakken, O., et al. (2011). Bottom trawl surveys. In *The Barents Sea: ecosystem, resources, management: Half a century of Russian-Norwegian cooperation* (ed. Jakobsen, T.). Tapir Academic Press, Trondheim, pp. 570–583.
- Pinceel, T., Vanschoenwinkel, B., Brendonck, L. & Buschke, F. (2016). Modelling the sensitivity of life history traits to climate change in a temporary pool crustacean. *Sci. Rep.*, 6, 1–5.
- R Core Team (2018). *R: A Language and Environment for Statistical Computing*. R Foundation for Statistical Computing, Vienna, Austria.
- Ranta, E. (1997). The spatial dimension in population fluctuations. *Science* (80-), 278(5343), 1621–1623.
- Ranta, E., Lundberg, P. & Kaitala, V. (2006). *Ecology of Populations*. Cambridge University Press, Cambridge.
- Royama, T. (1977). Population persistence and density dependence. *Ecol. Monogr.*, 47, 1–35.
- Ruokolainen, L. (2013). Spatio-temporal environmental correlation and population variability in simple metacommunities. *PLoS ONE*, 8, e72325.
- Sæther, B.-E. (1997). Environmental stochasticity and population dynamics of large herbivores: a search for mechanisms. *Trends Ecol. Evol.*, 12, 143–147.
- Sæther, B.-E. & Bakke, O. (2000). Avian life history variation and contribution of demographic traits to the population growth rate. *Ecology*, 81, 642.
- Sæther, B.-E., Ringsby, T.H., Røskift, E., Saether, B.-E. & Roskift, E. (1996). Life history variation, population processes and priorities in species conservation: towards a reunion of research paradigms. *Oikos*, 77, 217–226.
- Sæther, B.-E., Engen, S., Grøtan, V., Fiedler, W., Matthysen, E., Visser, M.E. et al. (2007). The extended Moran effect and large-scale synchronous fluctuations in the size of great tit and blue tit populations. *J. Anim. Ecol.*, 76, 315–325.
- Shelton, A.O. & Mangel, M. (2011). Fluctuations of fish populations and the magnifying effects of fishing. *Proc. Natl Acad. Sci.*, 108, 7075–7080.
- Shestakova, T.A., Gutiérrez, E., Kirdyanov, A.V., Camarero, J.J., Génova, M., Knorre, A.A. et al. (2016). Forests synchronize their growth in contrasting Eurasian regions in response to climate warming. *Proc. Natl Acad. Sci.*, 113, 662–667.
- Shine, R. & Charnov, E.L. (1992). Patterns of survival, growth, and maturation in snakes and lizards. *Am. Nat.*, 139, 1257–1269.
- Söndgerath, D. & Schröder, B. (2002). Population dynamics and habitat connectivity affecting the spatial spread of populations – a simulation study. *Landsc. Ecol.*, 17, 57–70.
- Stiansen, J.E. & Filin, A.A. (Eds.) (2008). Joint PINRO/IMR Report on the state of the Barents Sea ecosystem in 2007, with expected situation and considerations for Management. IMR-PINRO Jt. Rep. Ser. 2008 (1). Bergen, Norway.
- Swain, D.P., Benoît, H.P. & Hammill, M.O. (2015). Spatial distribution of fishes in a Northwest Atlantic ecosystem in relation to risk of predation by a marine mammal. *J. Anim. Ecol.*, 84, 1286–1298.
- Thorson, J.T., Munch, S.B., Cope, J.M. & Gao, J. (2017). Predicting life history parameters for all fishes worldwide. *Ecol. Appl.*, 27, 2262–2276.
- Vasseur, D.A. & Fox, J.W. (2009). Phase-locking and environmental fluctuations generate synchrony in a predator-prey community. *Nature*, 460, 1007–1010.
- Walter, J.A., Sheppard, L.W., Anderson, T.L., Kastens, J.H., Bjørnstad, O.N., Liebhold, A.M. et al. (2017). The geography of spatial synchrony. *Ecol. Lett.*, 20, 801–814.
- Winemiller, K.O. & Rose, K.A. (1992). Patterns of life-history diversification in North American fishes: implications for population regulation. *Can. J. Fish. Aquat. Sci.*, 49, 2196–2218.
- Yaragina, N.A. & Dolgov, A.V. (2009). Ecosystem structure and resilience-A comparison between the Norwegian and the Barents Sea. *Deep Sea Res. Part II Top. Stud. Oceanogr.*, 56, 2141–2153.

## SUPPORTING INFORMATION

Additional supporting information may be found online in the Supporting Information section at the end of the article.

Editor, Stephan Munch

Manuscript received 27 May 2019

Manuscript accepted 29 June 2019